JOURNAL OF GUIDANCE, CONTROL, AND DYNAMICS
Vol. 37, No. 2, March–April 2014

# Flight Control of a Quadrotor Vehicle Subsequent to a Rotor Failure

Alexander Lanzon*
*University of Manchester, Manchester, England M13 9PL, United Kingdom*
and
Alessandro Freddi† and Sauro Longhi‡
*Università Politecnica delle Marche, 60131 Ancona, Italy*

DOI: 10.2514/1.59869

**In this paper, the problem of designing a control law in case of rotor failure in quadrotor vehicles is addressed. First, a nonlinear mathematical model for a quadrotor vehicle is derived, which includes translational and rotational dynamics. Then a robust feedback linearization controller is developed, which sacrifices the controllability of the yaw state due to rotor failure to linearize the closed-loop system around a working point, where roll and pitch angles are zero and the angular speed around the vertical axis is a nonzero constant. An $H_\infty$ loop shaping technique is adopted to achieve regulation of these variables around the chosen working point. Finally, an outer loop is proposed for achieving control of the linear displacement under the assumption of small angles approximation for the pitch and roll angles. The proposed control strategy allows the vehicle to use the remaining three functional rotors to enter a constant angular speed around its vertical axis, granting stability and representing an effective way to deal with a rotor failure in quadrotor vehicles.**



## Nomenclature

| | | |
|---|---|---|
| $d$ | = | ratio between drag and thrust coefficients of a rotor, m |
| $f_j$ | = | thrust force provided by the $j$th rotor, N |
| $f_{\max}$ | = | upper bound on thrust force, N |
| $f_{\min}$ | = | lower bound on thrust force, N |
| $g$ | = | gravity acceleration, 9.81 m/s$^2$ |
| $\boldsymbol{I}$ | = | inertia matrix, kg · m$^2$ |
| $I_{xx}, I_{yy}, I_{zz}$ | = | principal moments of inertia, kg · m$^2$ |
| $k_r$ | = | rotational drag, N · m · s |
| $k_t$ | = | linear drag, N · s/m |
| $l$ | = | arm length, m |
| $m$ | = | quadrotor total mass, kg |
| $p$ | = | rotational speed around $x_B$ axis, rad/s |
| $q$ | = | rotational speed around $y_B$ axis, rad/s |
| $\{R\}(O, x, y, z)$ | = | frame attached to the Earth |
| $\{R_B\}(O_B, x_B, y_B, z_B)$ | = | frame attached to the body |
| $r$ | = | rotational speed around $z_B$ axis, rad/s |
| $u_f$ | = | total upward lift force provided by the blades, N |
| $\boldsymbol{\eta}$ | = | quadrotor attitude with respect to Earth frame, rad |
| $\theta$ | = | pitch angle, rad |
| $\xi$ | = | quadrotor position with respect to Earth frame, m |
| $\boldsymbol{\tau}_B$ | = | torque vector around body frame axes, N · m |
| $\tau_p, \tau_q, \tau_r$ | = | torque vector components due to actuation forces for axes $x_B$, $y_B$, and $z_B$, N · m |
| $\phi$ | = | roll angle, rad |
| $\psi$ | = | yaw angle, rad |

Received 7 August 2012; revision received 16 March 2013; accepted for publication 29 July 2013; published online 12 February 2014. 

*Control Systems Centre, School of Electrical and Electronic Engineering, Sackville Street; Alexander.Lanzon@manchester.ac.uk.

†Department of Information Engineering, Via Brecce Bianche; freddi@dii.univpm.it.

‡Department of Information Engineering, Via Brecce Bianche; sauro.longhi@univpm.it.

## I. Introduction

QUADROTORS, also called quadcopters, are small aerial vehicles propelled by four rotors. They are commonly designed to be used as unmanned aerial vehicles: vehicles that can accomplish a task without the aid of a human guide. They present several advantages with respect to comparable scale helicopters. First, the four rotors generate a vertical lift thrust, which, combined with the symmetrical geometry, allows this kind of vehicle to be highly maneuverable. Second, the use of four rotors ensures that individual rotors are smaller in diameter than the equivalent main rotor on a helicopter, relative to the airframe size. In this way, the damage caused by the blades in case of collision is reduced; moreover, by enclosing the rotors within a frame, the rotors can be protected during collisions, permitting flight indoor and in obstacle-dense environments, with low risk of damaging the vehicle, its operators, or its surroundings [1]. Third, quadrotors are based on fixed rotor blade pitch angles and vary their attitude by changing the rotational speed of each rotor: this simplifies the mechanical design of the vehicle and reduces maintenance time and cost. High maneuverability, safety, and simplicity have made the quadrotor one of the most interesting aerial vehicles for indoor/outdoor navigation [2].

Despite different prototypes, control algorithms, and approaches, all the quadrotor architectures have an increased risk of motor/rotor failure, with respect to similar vehicles with a reduced number of motors/rotors. The main contribution of this paper is to successfully develop a control law that can be applied in case of loss of one of the actuators (i.e., rotors), to stabilize a subset of the attitude dynamics of the quadrotor, which is sufficient to maintain controlled flight and make the quadrotor fly to any desired position in three-dimensional (3-D) space (usually a specified point on the ground).

Several control approaches have been presented in the literature for a fault-free quadrotor vehicle. Dynamic inversion and feedback linearization techniques have been proposed by many authors, using different models [3,4]: The attitude of the quadrotor vehicle can be controlled, however, the lack of robustness is a common defect. Robustness in unmanned aerial vehicles [5–7] can be achieved using different approaches. In [8,9], a nonlinear control law based on a nested saturations technique is presented that stabilizes the state of the quadrotor vehicle around the origin: This approach is robust against saturation, however, it is valid only for near-hover flight.

Nonlinear techniques can be applied in a wide range of operating points: In [10], a comparison between classical feedback linearization techniques and sliding mode control for the quadrotor is performed, whereas in [11], backstepping is adopted to increase robustness. Recently, $H_\infty$ and model predictive control (MPC) [12,13] have been often adopted to control the quadrotor, because they grant both good performances and robustness properties.

Only few approaches have been proposed in the literature to deal with actuator faults for the quadrotor vehicle: feedback linearization [14], sliding mode [15], and MPC [16]. These approaches, however, consider only a partial loss of control effectiveness and do not address the problem of total failure of one of the rotors.

To the best of the authors' knowledge, however, the control problem in case of total loss of one of the rotors has never been addressed before for the quadrotor vehicle. Robust feedback linearization [17] has been chosen to deal with the problem of controlling the quadrotor vehicle when one of the actuators (rotors) is lost. The reason is that this technique provides a systematic multi-input/multi-output method to handle dynamics robustly, and it proved to be effective to control a quadrotor vehicle when all the actuators (rotors) are working [18].

The challenging aspect of the proposed problem is in the impossibility to maintain full control of all the attitude states and all the translational states when a primary actuator (i.e., a rotor) has failed and the system becomes underactuated. This paper proposes a solution to this loss of control action by spinning the vehicle in the yaw direction, thereby maintaining flight control of a spinning vehicle.

Flight control is achieved through robust feedback linearization which linearizes the nonlinear system around an operating point where roll and pitch angles are zero but the angular speed around the vertical axis is a nonzero constant. The closed-loop linearized system is controlled through an $H_\infty$ loop shaping technique, which performs regulation around the chosen working point. Finally, an outer control loop is proposed to achieve control of the linear displacement under the assumption of small angles approximation for the pitch and roll angles. Thus, the inner attitude control loop handles robustness considerations and the failure of a primary actuator, and the outer loop enables translationary flight control to take the vehicle down safely at an arbitrary location.

From a theoretical point of view, there may be solutions that enable a single control law to be designed, thereby avoiding an inner-/outer-loop architecture. Although some such techniques appear in the literature for the fault-free case (i.e., when all four rotors are fully functional), no such methods exist for an underactuated system as considered in this paper. Additionally, the authors argue that this inner-/outer-loop decoupling is natural from a practical point of view because it achieves robust nonlinear attitude control in the inner loop and slow/low bandwidth translation time-varying (cyclic oscillatory) control in the outer loop.

The paper is organized as follows. In Sec. II, the nonlinear model of the quadrotor is presented. Section III contains the mathematical formulation of the control laws. Section IV is devoted to the presentation of the simulation results obtained when the proposed solution is applied to the quadrotor. Conclusions are presented at the end of the paper.

## II. Quadrotor Model

A quadrotor simply consists of four dc motors on which propellers are fixed. These motors are arranged to the extremities of an X-shaped frame, where all the arms make an angle of 90 deg with one another. As shown in Fig. 1, the front and rear motors $\mathcal{M}_1$ and $\mathcal{M}_3$ spin in the clockwise direction with angular velocities $\boldsymbol{\omega}_1$ and $\boldsymbol{\omega}_3$, whereas the other two rotors $\mathcal{M}_2$ and $\mathcal{M}_4$ spin in the counterclockwise direction with angular velocities $\boldsymbol{\omega}_2$ and $\boldsymbol{\omega}_4$.

### A. Control Model

Most of the approaches available in the literature consider the quadrotor as a rigid body subject to forces and moments [1,11,19–23]. The nominal mathematical model (i.e., the model that will be used to derive the control laws in Sec. III) is based on this approximation and on the following assumptions:

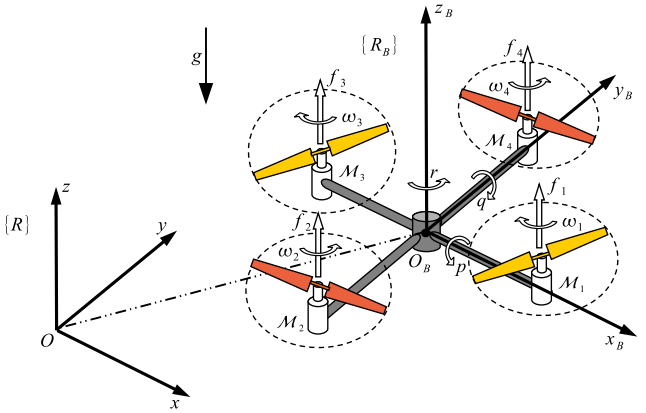


**Fig. 1 Quadrotor scheme used for the development of the mathematical model.**

1) The quadrotor design is symmetrical in the horizontal plane; in this way, the inertia along the longitudinal axis is assumed to be the same as that of the lateral axis.

2) Propellers are considered rigid, thus blade flapping is not considered in the model.

3) Drag is assumed to be linear, thus obeying Stokes' law.

These assumptions are usually valid for quadrotors because they are built with horizontal symmetry and have small propellers [8].

Two frames are used to study the system motion: a frame attached to the Earth $\{R\}(O, x, y, z)$, which is assumed to be inertial, and a body-fixed frame $\{R_B\}\{O_B, x_B, y_B, z_B\}$, where $O_B$ is fixed to the center of mass of the quadrotor. The body-fixed frame $\{R_B\}$ is related to $\{R\}$ by a position vector $\xi = [x \quad y \quad z]^T$, describing the position of the center of gravity in $\{R_B\}$ relative to $\{R\}$ and by a vector of three independent angles $\boldsymbol{\eta} = [\phi \quad \theta \quad \psi]^T$, which represent the orientation of the body-fixed frame $\{R_B\}\{O_B, x_B, y_B, z_B\}$ with respect to the Earth frame $\{R\}(O, x, y, z)$. The adopted notation, usually called yaw, pitch, and roll, is based on the assumption that the Earth frame $\{R\}(O, x, y, z)$ can reach the same orientation of the body-fixed frame $\{R_B\}\{O_B, x_B, y_B, z_B\}$ by first performing a rotation of an angle $\psi$ around the $z$ axis (yaw), then a rotation of an angle $\theta$ around the new $y$ axis (pitch), and finally a rotation of an angle $\phi$ around the new $x$ axis (roll). All the rotations are right handed with

$$\left(-\frac{\pi}{2} < \phi < \frac{\pi}{2}\right), \qquad \left(-\frac{\pi}{2} < \theta < \frac{\pi}{2}\right)$$

and $\psi$ is unrestricted (see Fig. 1). This implies that the vehicle must not perform acrobatic maneuvers: The heading of the quadrotor can vary freely, but the roll and pitch angles cannot assume a value such that the vehicle undergoes inverted flight. This assumption is valid in almost any application field of the quadrotor vehicle (e.g., surveillance, low-cost photogrammetry). In this way, $\xi$ and $\boldsymbol{\eta}$ fully describe, respectively, the translational and the rotational movement of the rotorcraft with respect to the Earth frame.

The dynamics of the quadrotor can be described analyzing the forces acting on it, which are the weight force, the thrust forces, and the drag terms. The weight force is applied to the center of gravity and directed along the negative $z$ axis in the Earth frame. The thrust force $\boldsymbol{f}_j$, where $j = 1, 2, 3, 4$, is applied to the center of the $j$th motor, distant $l$ from the center of mass, and directed along the positive $z_B$ axis because blade flapping is neglected: $f_j \geq 0$ for $j = 1, \ldots, 4$. The imbalance of the forces $\boldsymbol{f}_j$, where $j = 1, 3$ or $j = 2, 4$, results in torques, along a direction perpendicular to the plane containing the forces $\boldsymbol{f}_j$ for $j = 1, 3$ or $j = 2, 4$. This torque is responsible for the rotation of the quadrotor along the $y_B$ and $x_B$ axes. The rotation about the $z_B$ axis is due to imbalance of clockwise and counterclockwise drag reaction torques. The drag terms on the vehicle body obey Stokes' law: The translational drag is proportional to the linear velocity and the rotational drag term is proportional to the angular

velocity with coefficients $k_t$ and $k_r$ assumed to be equal in all directions for simplicity.

Denote with $m$ the whole mass of the rotorcraft and define the inertia matrix in the body frame, which is symmetric by assumption, as

$$\boldsymbol{I} \doteq \begin{bmatrix} I_{xx} & 0 & 0 \\ 0 & I_{yy} & 0 \\ 0 & 0 & I_{zz} \end{bmatrix} \tag{1}$$

The force due to the control inputs, expressed into the body frame, has a nonzero component in the $z_B$ direction only: $u_f = f_1 + f_2 + f_3 + f_4$.

Denoting with $p$, $q$, and $r$ the instantaneous angular speeds around the $x_B$, $y_B$, and $z_B$ axes, respectively, the actuation torques around the body frame axes are described by

$$\boldsymbol{\tau}_B = \begin{bmatrix} \tau_p \\ \tau_q \\ \tau_r \end{bmatrix} = \begin{bmatrix} l(f_4 - f_2) \\ l(f_3 - f_1) \\ d(f_1 - f_2 + f_3 - f_4) \end{bmatrix} \tag{2}$$

where $l$ is the arm length and $d$ is the ratio between the drag and the thrust coefficients of the blade. Using the well-known rigid-body equations, with the Newton–Euler formalism [24], the complete model can be expressed as [25]

$$\begin{cases} \ddot{x} = \frac{1}{m}[(C_\phi C_\psi S_\theta + S_\phi S_\psi)u_f - k_t \dot{x}] \\ \ddot{y} = \frac{1}{m}[(C_\phi S_\theta S_\psi - C_\psi S_\phi)u_f - k_t \dot{y}] \\ \ddot{z} = \frac{1}{m}[(C_\theta C_\phi)u_f - mg - k_t \dot{z}] \\ \dot{p} = \frac{1}{I_{xx}}[-k_r p - qr(I_{zz} - I_{yy}) + \tau_p] \\ \dot{q} = \frac{1}{I_{yy}}[-k_r q - pr(I_{xx} - I_{zz}) + \tau_q] \\ \dot{r} = \frac{1}{I_{zz}}[-k_r r - pq(I_{yy} - I_{xx}) + \tau_r] \\ \dot{\phi} = p + qS_\phi T_\theta + rC_\phi T_\theta \\ \dot{\theta} = qC_\phi - rS_\phi \\ \dot{\psi} = \frac{1}{C_\theta}[qS_\phi + rC_\phi] \end{cases} \tag{3}$$

where $S_{(.)}$, $C_{(.)}$, and $T_{(.)}$ denote $\sin(.)$, $\cos(.)$, and $\tan(.)$, respectively. In Eqs. (3), the system inputs are $u_f$, $\tau_p$, $\tau_q$, and $\tau_r$, whereas the real inputs of the system are $f_1$, $f_2$, $f_3$, and $f_4$: this is without loss of generality because the relation

$$\begin{bmatrix} u_f \\ \tau_p \\ \tau_q \\ \tau_r \end{bmatrix} = \begin{bmatrix} 1 & 1 & 1 & 1 \\ 0 & -l & 0 & l \\ -l & 0 & l & 0 \\ d & -d & d & -d \end{bmatrix} \begin{bmatrix} f_1 \\ f_2 \\ f_3 \\ f_4 \end{bmatrix} \tag{4}$$

is bijective.

### B. Verification Model

Although it is necessary to adopt a simplified nominal mathematical model for control purposes, robustness to unmodeled dynamics should be at the foreground of any consideration when designing any control law. For this reason, a more comprehensive model will be used for testing purposes in Sec. IV, to show the robustness of the proposed solution. More in detail, the verification model will include the following effects.

1) Blade gyroscopic effect: The gyroscopic moment generated by the different rotational speeds of the propellers is typically neglected when all the rotors are properly working, however, it may become significant in case of rotor failure. The effect has been modeled as an additional moment, according the following equation [11,26]:

$$\boldsymbol{m}_g = I_R(\boldsymbol{\Omega} \times [0 \quad 0 \quad 1]^T)(\omega_1 + \omega_3 - \omega_2 - \omega_4) \tag{5}$$

where $\boldsymbol{\Omega}$ is the angular velocity of the body read into the body frame and $I_R$ is the propeller inertia.

2) Actuator saturation: From a physical point of view, the rotation speed of each motor is limited, therefore, there is an upper bound to the values of each thrust: $f_j \leq f_{\max}$ for $j = 1, \ldots, 4$.

3) Actuator rate limiting: From a physical point of view, each rotor needs a certain time to achieve a desired rotational speed, therefore, there is an upper bound (and lower bound) to the variation of each thrust: $-\Delta f \leq \dot{f}_j \leq \Delta f$ for $j = 1, \ldots, 4$.

## III. Control Architecture

In the literature, several techniques have been proposed to control a quadrotor vehicle with all rotors functional: dynamic inversion [3,4], nested saturations [8], nonlinear $H_\infty$ control, MPC [12], feedback linearization [10], and backstepping [11] are among the most used approaches. Usually the control strategy is based upon a double-loop architecture. An inner and faster controller has the task to regulate the attitude angles and the altitude of the vehicle acting independently of the three torques, but depends on the total lift thrust. An outer and slower controller has instead the aim of modifying the desired values of $\phi$ and $\theta$ by small angles to perform trajectory following.

The controller developed here, however, is based on the assumption that one of the four actuators has failed (no longer able to provide an upward lift force), while the other three actuators are still fully functional. For this reason, the objective of this controller is no longer that of allowing the vehicle to continue its mission, but rather to safely recover it. When one of the rotors fails, indeed, the quadrotor loses the ability to control independently the three torques necessary to fully control the attitude of the vehicle. This typically results in a vehicle losing attitude control, then losing translational control, and then finally crashing. This rotor failure implies the loss of controllability of one variable from roll, pitch, yaw, and altitude. Most papers in the literature [5,6,27] argue that, without full attitude control, flight control cannot be achieved. The authors aim to show that this statement is not necessarily correct, as one can control a subset of attitude dynamics and still be able to fly the vehicle, albeit spinning at a constant angular speed in the yaw dynamics. It is the authors' opinion that, from a physical point of view, the most important variables to control are roll, pitch, and altitude for an unmanned aerial vehicle. The roll and pitch angles are of vital importance because a small change in their values results in a big change in the longitudinal/lateral displacement in the Earth frame. On the other hand, altitude must always be kept above a positive threshold to avoid collision with the ground. The impossibility to control yaw displacement when a rotor failure occurs, instead, implies loosing the heading of the vehicle, which is only important whenever the vehicle must accomplish tasks that require directional sensors (e.g., cameras, lasers, etc.), but may be considered of minor importance when dealing with a safe landing procedure. For these reasons, the control law proposed in this paper is developed sacrificing the controllability of the yaw state.

The control structure can still be realized using the double-loop architecture already mentioned, however, it must be modified (see Fig. 2). When the quadrotor is flying using only three rotors, the unbalance in the propeller drag makes it to spin around its vertical axis. Increasing the rotational speed of the blades (that is to say, increasing the upward lift force $u_f$) causes the vehicle to increase its altitude and also to spin faster in the yaw direction. Basically, the rotational speed around the quadrotor vertical axis and the altitude variation depends on the same input and are hence coupled. This property is exploited in the control law architecture: The inner control loop controls roll and pitch angles and yaw rotational speed, whereas the outer control loop sets the desired values of the $\phi$ and $\theta$ angles to control position in the $xy$ plane. Furthermore, the desired altitude can be obtained by changing the set point in the yaw rotational speed. Because roll, pitch, and altitude have the highest priority during unmanned vehicle flight, the inner controller works much faster than the outer controller and the inner control loop is specifically designed for robustness. All the quadrotor states must be accessible to develop the controller: The inner controller needs the states $[\phi, \theta, \psi, p, q, r]$, whereas $[x, y, z]$ are only needed by the outer control loop. Even if the knowledge of $\psi$ is requested to control the quadrotor, the

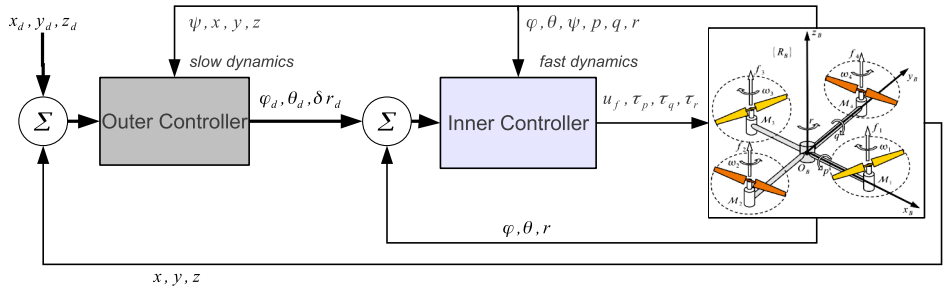


**Fig. 2 Control system scheme: the double-loop architecture in case of actuator loss.**

controllability of the $\psi$ state is sacrificed because the vehicle is underactuated.

### A. Quadrotor Model in Case of Actuator Loss

Fault detection and isolation (FDI) of actuator faults in quadrotor vehicles is out of the scope of the present paper. However, it is relevant to mention that a wide class of model-based algorithms [28] can be applied to the quadrotor vehicle to perform FDI, and several papers in the literature have already tackled this problem [29,30].

In this section, the case of failure on actuator 2 is described. Because of the symmetry of the system, a similar controller can be easily developed in case of failure on actuators 1, 3, or 4 using the same principles. In case of failure on $\mathcal{M}_2$, the control inputs are chosen as $u_f$, $\tau_q$, and $\tau_r$ (i.e., $\tau_p$ is no longer used as a direct control input) so that the relation

$$\begin{bmatrix} u_f \\ \tau_q \\ \tau_r \end{bmatrix} = \begin{bmatrix} 1 & 1 & 1 \\ -l & l & 0 \\ d & d & -d \end{bmatrix} \begin{bmatrix} f_1 \\ f_3 \\ f_4 \end{bmatrix} \tag{6}$$

is again bijective. The constraints on the real inputs, which are

$$\begin{cases} f_j \geq 0, & j = 1,3,4 \\ f_j \leq f_{\max}, & j = 1,3,4 \end{cases} \tag{7}$$

must be reexpressed as constraints on the inputs $u_f$, $\tau_q$, and $\tau_r$. The constraints $f_j \geq 0$ for $j = 1,3,4$ are equivalent to

$$\begin{cases} |\tau_q| \leq \frac{l}{2}\left(u_f + \frac{\tau_r}{d}\right), \\ |\tau_r| \leq d u_f \end{cases} \tag{8}$$

This is because

$$\begin{bmatrix} f_1 \\ f_3 \\ f_4 \end{bmatrix} = \frac{1}{4} \begin{bmatrix} 1 & -\frac{2}{l} & \frac{1}{d} \\ 1 & \frac{2}{l} & \frac{1}{d} \\ 2 & 0 & -\frac{2}{d} \end{bmatrix} \begin{bmatrix} u_f \\ \tau_q \\ \tau_r \end{bmatrix} \tag{9}$$

yields

$$\begin{cases} u_f - \frac{2\tau_q}{l} + \frac{\tau_r}{d} \geq 0 \\ u_f + \frac{2\tau_q}{l} + \frac{\tau_r}{d} \geq 0 \\ 2u_f - \frac{2\tau_r}{d} \geq 0 \end{cases} \tag{10}$$

when imposing $f_j \geq 0$ for $j = 1,3,4$, which then is equivalent to Eq. (8). Furthermore, $f_j \leq f_{\max}$ for $j = 1,3,4$ implies $u_f \leq 3f_{\max}$: This follows from Eq. (6) imposing $f_j \leq f_{\max}$ for $j = 1,3,4$.

In a similar way, the constraints due to the rate limiters can be written as

$$\begin{cases} -\Delta f \leq \frac{1}{4}\dot{u}_f - \frac{\dot{\tau}_q}{2l} + \frac{\dot{\tau}_r}{4d} \leq \Delta f \\ -\Delta f \leq \frac{1}{4}\dot{u}_f + \frac{\dot{\tau}_q}{2l} + \frac{\dot{\tau}_r}{4d} \leq \Delta f \\ -\Delta f \leq \frac{1}{2}\dot{u}_f - \frac{\dot{\tau}_r}{2d} \leq \Delta f \end{cases} \tag{11}$$

Choosing the state vector as

$$\begin{aligned} \boldsymbol{x} &= [x_1 \quad x_2 \quad x_3 \quad x_4 \quad x_5 \quad x_6 \quad x_7 \quad x_8 \quad x_9 \quad x_{10} \quad x_{11} \quad x_{12}]^T \\ &= [\phi \quad \theta \quad \psi \quad p \quad q \quad r \quad x \quad y \quad z \quad \dot{x} \quad \dot{y} \quad \dot{z}]^T \end{aligned} \tag{12}$$

and the input vector as

$$\boldsymbol{u} = [u_1 \quad u_2 \quad u_3]^T = [u_f \quad \tau_q \quad \tau_r]^T \tag{13}$$

then the set of Eq. (3) can be written in state-space form as

$$\dot{x}_1 = x_4 + x_5 S_{x_1} T_{x_2} + x_6 C_{x_1} T_{x_2} \tag{14a}$$

$$\dot{x}_2 = x_5 C_{x_1} - x_6 S_{x_1} \tag{14b}$$

$$\dot{x}_3 = \frac{1}{C_{x_2}}[x_5 S_{x_1} + x_6 C_{x_1}] \tag{14c}$$

$$\dot{x}_4 = \frac{1}{I_{xx}}\left[-k_r x_4 - x_5 x_6 (I_{zz} - I_{xx}) + \frac{l}{2}\left(u_1 - \frac{u_3}{d}\right)\right] \tag{14d}$$

$$\dot{x}_5 = \frac{1}{I_{xx}}[-k_r x_5 - x_4 x_6 (I_{xx} - I_{zz}) + u_2] \tag{14e}$$

$$\dot{x}_6 = \frac{1}{I_{zz}}(-k_r x_6 + u_3) \tag{14f}$$

$$\dot{x}_7 = x_{10} \tag{14g}$$

$$\dot{x}_8 = x_{11} \tag{14h}$$

$$\dot{x}_9 = x_{12} \tag{14i}$$

$$\dot{x}_{10} = \frac{C_{x_1} S_{x_2} C_{x_3} + S_{x_1} S_{x_3}}{m} u_1 - \frac{k_t}{m} x_{10} \tag{14j}$$

$$\dot{x}_{11} = \frac{C_{x_1} S_{x_2} S_{x_3} - S_{x_1} C_{x_3}}{m} u_1 - \frac{k_t}{m} x_{11} \tag{14k}$$

$$\dot{x}_{12} = \frac{1}{m}[u_1 C_{x_1} C_{x_2} - k_t x_{12} - mg] \tag{14l}$$

in which $I_{xx}$ has been chosen equal to $I_{yy}$ due to the symmetry of the quadrotor. Note that, in Eq. (14d), $\tau_p = l f_4$ via Eq. (4) since $f_2 = 0$ and

$$f_4 = \frac{1}{4}\left(2u_1 - \frac{2u_3}{d}\right)$$

via Eq. (9).

### B. Robust Feedback Linearization: Definitions and Main Results

Consider a nonlinear system with $n$ states, $m$ inputs, and $m$ outputs described by the state-space equations

$$\dot{\boldsymbol{x}} = \boldsymbol{f}(\boldsymbol{x}) + \boldsymbol{G}(\boldsymbol{x})\boldsymbol{u} = \boldsymbol{f}(\boldsymbol{x}) + \sum_{i=1}^{m} \boldsymbol{g}_j(\boldsymbol{x})u_j \tag{15a}$$

$$\boldsymbol{y} = [\,h_1(\boldsymbol{x}),\ \ldots,\ h_m(\boldsymbol{x})\,]^T \tag{15b}$$

where $\boldsymbol{x} \in \mathbb{R}^n$ denotes the state vector, $\boldsymbol{u} \in \mathbb{R}^m$ is the control input, $\boldsymbol{y} \in \mathbb{R}^m$ is the output vector, and $\boldsymbol{f}(\boldsymbol{x})$, $\boldsymbol{g}_1(\boldsymbol{x})$, $\ldots$, $\boldsymbol{g}_m(\boldsymbol{x})$, $\boldsymbol{y}$ are smooth vector fields defined on an open subset of $\mathbb{R}^n$.

Suppose that system (15) satisfies the well-known conditions for feedback linearization [31]: The relative degree of $h_i$ is equal to $r_i$ $\forall\ i = 1, \ldots, m$ such that $r_1 + \cdots + r_m = n$, and the decoupling matrix

$$\boldsymbol{M}(\boldsymbol{x}) = \begin{bmatrix} L_{g_1}L_f^{r_1-1}h_1(\boldsymbol{x}) & \ldots & L_{g_m}L_f^{r_1-1}h_1(\boldsymbol{x}) \\ L_{g_1}L_f^{r_2-1}h_2(\boldsymbol{x}) & \ldots & L_{g_m}L_f^{r_2-1}h_2(\boldsymbol{x}) \\ \ldots & \ldots & \ldots \\ L_{g_1}L_f^{r_m-1}h_m(\boldsymbol{x}) & \ldots & L_{g_m}L_f^{r_m-1}h_m(\boldsymbol{x}) \end{bmatrix} \tag{16}$$

is invertible, where $L_{(.)}(.)$ denotes the Lie derivative operator. It is then possible to find a linearizing control law of the form

$$\boldsymbol{u}(\boldsymbol{x}, \boldsymbol{w}) = \boldsymbol{\alpha}_c(\boldsymbol{x}) + \boldsymbol{\beta}_c(\boldsymbol{x})\boldsymbol{w} \tag{17}$$

where $\boldsymbol{w}$ is a linear control input and the change of coordinates is defined by a diffeomorphism as $\boldsymbol{x}_c = \boldsymbol{\phi}_c(\boldsymbol{x})$. This control law reduces the nonlinear system (15) into a linear system of the form

$$\dot{\boldsymbol{x}}_c = \boldsymbol{A}_c\boldsymbol{x}_c + \boldsymbol{B}_c\boldsymbol{w} \tag{18}$$

where $\boldsymbol{A}_c$, $\boldsymbol{B}_c$ are the matrices of the canonical Brunowski form.

The robust feedback linearization, instead, brings the system in the Jacobian approximation around the origin rather than in the Brunowski form, that is to say,

$$\dot{\boldsymbol{x}}_r = \boldsymbol{A}_r\boldsymbol{x}_r + \boldsymbol{B}_r\boldsymbol{v} \tag{19}$$

where $\boldsymbol{A}_r = \partial_x\boldsymbol{f}(0)$ and $\boldsymbol{B}_r = \boldsymbol{G}(0)$. In this case, the original nonlinear system is only minorly transformed, which makes it more probable that the properties of the linear design (including robustness) still hold for the nonlinear closed loop. In this way, the original nonlinear system is reduced to a linear system that is equivalent to its Jacobian linearization around the origin, which can then be controlled using well-known linear techniques. Indeed [17,32] have shown that, when the nonlinear system (15) is transformed to its Jacobian linearization (31), robustness in the sense of $H_\infty$ loop shaping on Eq. (31) is preserved on the original nonlinear system (15).

The linearizing control law in this case has the form

$$\boldsymbol{u}(\boldsymbol{x}, \boldsymbol{v}) = \boldsymbol{\alpha}(\boldsymbol{x}) + \boldsymbol{\beta}(\boldsymbol{x})\boldsymbol{v} \tag{20}$$

where

$$\boldsymbol{\alpha}(\boldsymbol{x}) = \boldsymbol{\alpha}_c(\boldsymbol{x}) + \boldsymbol{\beta}_c(\boldsymbol{x})\boldsymbol{L}\boldsymbol{T}^{-1}\boldsymbol{\phi}_c(\boldsymbol{x}) \tag{21a}$$

$$\boldsymbol{\beta}(\boldsymbol{x}) = \boldsymbol{\beta}_c(\boldsymbol{x})\boldsymbol{R}^{-1} \tag{21b}$$

$$\boldsymbol{\phi}(\boldsymbol{x}) = \boldsymbol{T}^{-1}\boldsymbol{\phi}_c(\boldsymbol{x}) \tag{21c}$$

$$\boldsymbol{L} = -\boldsymbol{M}(0)\partial_x\alpha_c(0) \tag{21d}$$

$$\boldsymbol{R} = \boldsymbol{M}^{-1}(0) \tag{21e}$$

$$\boldsymbol{T} = \partial_x\boldsymbol{\phi}_c(0) \tag{21f}$$

$$\boldsymbol{x}_r = \boldsymbol{\phi}(\boldsymbol{x}) \tag{21g}$$

### C. Control Loops

The control architecture is based on two control loops, each one acting on a subsystem.

1) The first subsystem includes the dynamics of the state variables $x_1, x_2, x_4, x_5, x_6$ and is controlled by a robust feedback linearization controller cascaded with an $H_\infty$ loop shaping linear controller.

2) The second subsystem includes the remaining dynamics [excluding Eq. (14c)]. Because the outer loop dynamics are slower than that of the inner loop, the longitudinal $x$ and lateral $y$ dynamics are controlled under the assumption of small angles for $\phi$ and $\theta$, whereas the vertical dynamics $z$ are controlled using variation of the yaw angular speed in the neighborhood of the operating point, which is chosen to achieve hover flight.

#### 1. Inner Control Loop

The robust feedback linearization is applied to the dynamics of roll, pitch, and yaw angular speed. Equations (14a), (14b), and (14d–14f) are written such that the origin of the system is an equilibrium point when the inputs are chosen to be zero. This is achieved by choosing

$$\hat{\boldsymbol{x}} = [\,\hat{x}_1 \quad \hat{x}_2 \quad \hat{x}_3 \quad \hat{x}_4 \quad \hat{x}_5\,] \doteq \left[\, x_1 \quad x_2 \quad x_4 \quad x_5 \quad \left(x_6 - \tfrac{mgd}{k_r}\right) \right] \tag{22a}$$

$$\hat{\boldsymbol{u}} = [\,\hat{u}_1 \quad \hat{u}_2 \quad \hat{u}_3\,] \doteq [\,(u_1 - mg) \quad u_2 \quad (u_3 - mgd)\,] \tag{22b}$$

The $\hat{\boldsymbol{x}}$ dynamics are given by

$$\dot{\hat{\boldsymbol{x}}} = \hat{\boldsymbol{f}}(\hat{\boldsymbol{x}}) + \hat{\boldsymbol{G}}(\hat{\boldsymbol{x}})\hat{\boldsymbol{u}} \tag{23a}$$

$$\hat{\boldsymbol{y}} \doteq [\,\hat{h}_1 \quad \hat{h}_2 \quad \hat{h}_3\,]^T = [\,\hat{x}_1 \quad \hat{x}_2 \quad \hat{x}_5\,]^T \tag{23b}$$

where

$$\hat{\boldsymbol{f}}(\hat{\boldsymbol{x}}) \doteq \begin{bmatrix} \hat{x}_3 + \hat{x}_4 S_{\hat{x}_1} T_{\hat{x}_2} + \left(\hat{x}_5 + \frac{mgd}{k_r}\right) C_{\hat{x}_1} T_{\hat{x}_2} \\ \hat{x}_4 C_{\hat{x}_1} - \left(\hat{x}_5 + \frac{mgd}{k_r}\right) S_{\hat{x}_1} \\ \frac{1}{I_{xx}}\left[-k_r\hat{x}_3 - \hat{x}_4\left(\hat{x}_5 + \frac{mgd}{k_r}\right)(I_{zz} - I_{xx})\right] \\ \frac{1}{I_{xx}}\left[-k_r\hat{x}_4 - \hat{x}_3\left(\hat{x}_5 + \frac{mgd}{k_r}\right)(I_{xx} - I_{zz})\right] \\ \frac{1}{I_{zz}}(-k_r\hat{x}_5) \end{bmatrix},$$

$$\hat{\boldsymbol{G}}(\hat{\boldsymbol{x}}) \doteq \begin{bmatrix} 0 & 0 & 0 \\ 0 & 0 & 0 \\ \frac{l}{2I_{xx}} & 0 & -\frac{l}{2dI_{xx}} \\ 0 & \frac{1}{I_{xx}} & 0 \\ 0 & 0 & \frac{1}{I_{zz}} \end{bmatrix} \tag{24}$$

The relative degrees are $r_1 = 2$, $r_2 = 2$, and $r_3 = 1$, resulting in a vector relative degree $r = 5$, which is equal to the number of states. The decoupling matrix can be written as

$$\boldsymbol{M}(\hat{\boldsymbol{x}}) = \begin{bmatrix} \frac{l}{2I_{xx}} & \frac{S_{\hat{x}_1} T_{\hat{x}_2}}{I_{xx}} & \frac{C_{\hat{x}_1} T_{\hat{x}_2}}{I_{zz}} - \frac{l}{2dI_{xx}} \\ 0 & \frac{C_{\hat{x}_1}}{I_{xx}} & \frac{-S_{\hat{x}_1}}{I_{zz}} \\ 0 & 0 & \frac{1}{I_{zz}} \end{bmatrix} \tag{25}$$

which is always invertible.

After calculating the classical Brunowski form linearizing input (17), and applying the formulas for the robust feedback linearization (21), the system can be robust feedback linearized into

$$\dot{\boldsymbol{x}}_r = \boldsymbol{A}_r \boldsymbol{x}_r + \boldsymbol{B}_r \boldsymbol{v}$$

where

$$\boldsymbol{A}_r = \begin{bmatrix} 0 & \frac{dgm}{k_r} & 1 & 0 & 0 \\ -\frac{dgm}{k_r} & 0 & 0 & 1 & 0 \\ 0 & 0 & -\frac{k_r}{I_{xx}} & \frac{dg(I_{xx}-I_{zz})m}{I_{xx}k_r} & 0 \\ 0 & 0 & -\frac{dg(I_{xx}-I_{zz})m}{I_{xx}k_r} & -\frac{k_r}{I_{xx}} & 0 \\ 0 & 0 & 0 & 0 & -\frac{k_r}{I_{zz}} \end{bmatrix} \tag{26a}$$

$$\boldsymbol{B}_r = \begin{bmatrix} 0 & 0 & 0 \\ 0 & 0 & 0 \\ \frac{l}{2I_{xx}} & 0 & -\frac{l}{2dI_{xx}} \\ 0 & \frac{1}{I_{xx}} & 0 \\ 0 & 0 & \frac{1}{I_{zz}} \end{bmatrix} \tag{26b}$$

The robust feedback linearizing control law (20) for system (23) is reported in the Appendix.

The linear input $v$ is then chosen using the $H_\infty$ loop shaping technique. The state variables $\hat{x}_1, \hat{x}_2, \hat{x}_5$ will be regulated to a desired set of small values around the chosen working point, $\phi_d$, $\theta_d$, and $\delta r_d$ as follows:

$$\hat{x}_1 = x_1 = \phi \to \phi_d \doteq x_{1,d} \tag{27a}$$

$$\hat{x}_2 = x_2 = \theta \to \theta_d \doteq x_{2,d} \tag{27b}$$

$$\hat{x}_5 = x_6 - \frac{mgd}{k_r} = r - \frac{mgd}{k_r} \to \delta r_d \doteq r_d - \frac{mgd}{k_r} \doteq x_{6,d} - \frac{mgd}{k_r} \tag{27c}$$

The scheme for controlling the dynamics of roll and pitch angles and yaw angular speed in case of actuator loss, based on robust feedback linearization and $H_\infty$ loop shaping, is shown in Fig. 3.

The target loop shape must be chosen to have large gain at low frequency (for small steady-state error), small gain at high frequency (for rejection to high-frequency noise and unmodeled dynamics), and does not roll off at a high rate near crossover (for good robustness) [33]. In this case, the resulting loop shape has 60 dB gain at low frequency, −40 dB/decade gain roll-off at high frequency, and −20 dB/decade slope near crossover frequency, which is set at 100 rad/s. The resulting loop shaping controller modifies the singular values of the closed-loop system, reducing the condition number between the values of the singular values of the shaped plant $P_s$ (see Fig. 4).

The proposed control loop causes roll and pitch angles and yaw angular speed to follow asymptotically the desired values. When the desired roll and pitch angles and variation of yaw rotational speed are chosen to converge to zero, the angular velocities $p$ and $q$ converge to zero and the angular velocity $r$ (and hence also the altitude) converges to a constant. As already stated, the only uncontrolled variable is the yaw angle, which is not relevant for stability, and whose controllability was sacrificed from the beginning to develop the proposed underactuated control law.

### 2. *Outer Loop*

The horizontal motion $(x, y)$ of the quadrotor depends on the direction that the horizontal component of the thrust vector, that is to say, the sum of the single thrusts of each rotor, assumes in this horizontal plane. Because this direction depends on the roll and pitch angles, it is possible to develop an outer control loop whose task is to generate the desired values for the roll and pitch angles to reach a desired position in the Earth-fixed frame. The vertical dynamics $z$ are controlled using a variation of the angular speed around the yaw axis in the neighborhood of the working point, which is set by the inner loop controller to achieve hover flight.

Assume that the inner control loop is robustly stabilizing and operating near the equilibrium ($x_1 \to x_{1,d}, x_2 \to x_{2,d}$, and $x_6 \to x_{6,d}$), the chosen desired values of $x_{1,d}$ and $x_{2,d}$ are small (i.e., the quadrotor is only required to make small adjustments to its attitude when one of the rotor is experiencing a failure) and the chosen desired value of $x_{6,d}$ is close to $mgd/k_r$ (i.e., the desired yaw spin speed is in the neighborhood of the equilibrium value, which is chosen proportional to the weight of the vehicle). From Eqs. (14a), (14b), and (14d–14f) follows that, at steady state, $u_3 \to x_{6,d} k_r$, $u_2 \to 0$, and

$$u_1 \to \frac{u_3}{d} = \frac{x_{6,d} k_r}{d}$$

when $x_{1,d} \to 0$ and $x_{2,d} \to 0$. Equations (14g–14l) can now be expressed as

$$\dot{x}_7 = x_{10} \tag{28a}$$

$$\dot{x}_8 = x_{11} \tag{28b}$$

$$\dot{x}_9 = x_{12} \tag{28c}$$

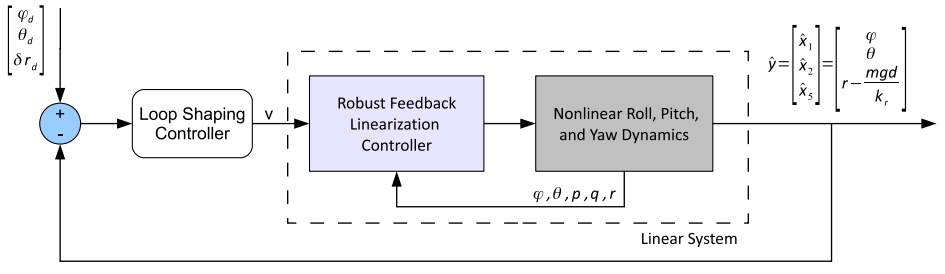


**Fig. 3 Scheme for the robust control law combining linear and nonlinear parts.**

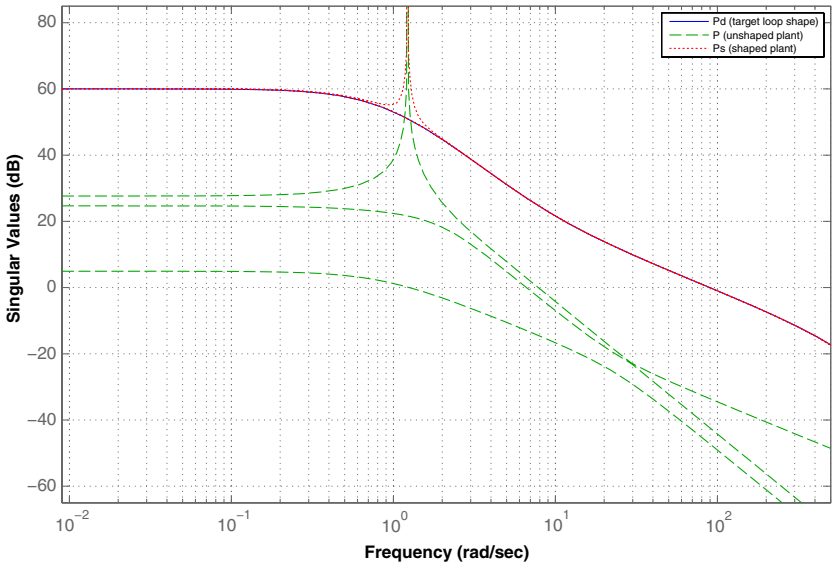


**Fig. 4 Singular values of the open-loop plant.**

$$\dot{x}_{10} = \frac{x_{2,d}C_{x_3} + x_{1,d}S_{x_3}}{m}\frac{k_r}{d}x_{6,d} - \frac{k_t}{m}x_{10} \tag{28d}$$

$$\dot{x}_{11} = \frac{x_{2,d}S_{x_3} - x_{1,d}C_{x_3}}{m}\frac{k_r}{d}x_{6,d} - \frac{k_t}{m}x_{11} \tag{28e}$$

$$\dot{x}_{12} = \frac{1}{m}\left[\frac{k_r}{d}x_{6,d} - k_t x_{12} - mg\right] \tag{28f}$$

using the assumptions of small angles for $x_{1,d}$ and $x_{2,d}$. Denoting with

$$\begin{aligned}\tilde{x} &\doteq [\,\tilde{x}_1 \quad \tilde{x}_2 \quad \tilde{x}_3 \quad \tilde{x}_4 \quad \tilde{x}_5 \quad \tilde{x}_6\,]^T \\ &\doteq [\,x_7 \quad x_8 \quad x_9 \quad x_{10} \quad x_{11} \quad x_{12}\,]^T\end{aligned} \tag{29a}$$

$$\tilde{\boldsymbol{u}} \doteq [\,\tilde{u}_1 \quad \tilde{u}_2 \quad \tilde{u}_3\,]^T \doteq \left[\frac{k_r x_{6,d}}{dm}x_{1,d} \quad \frac{k_r x_{6,d}}{dm}x_{2,d} \quad \frac{k_r x_{6,d}}{dm}\right]^T \tag{29b}$$

and remembering that $x_3 = \psi$ is measurable, then Eqs. (28a–28f) can be written as

$$\dot{\tilde{x}}_1 = \tilde{x}_4 \tag{30a}$$

$$\dot{\tilde{x}}_2 = \tilde{x}_5 \tag{30b}$$

$$\dot{\tilde{x}}_3 = \tilde{x}_6 \tag{30c}$$

$$\dot{\tilde{x}}_4 = C_\psi \tilde{u}_2 + S_\psi \tilde{u}_1 - \frac{k_t}{m}\tilde{x}_4 \tag{30d}$$

$$\dot{\tilde{x}}_5 = S_\psi \tilde{u}_2 - C_\psi \tilde{u}_1 - \frac{k_t}{m}\tilde{x}_5 \tag{30e}$$

$$\dot{\tilde{x}}_6 = \tilde{u}_3 - \frac{k_t}{m}\tilde{x}_6 - g \tag{30f}$$

As can be seen, the dynamics of longitudinal and lateral motion $(\tilde{x}_1, \tilde{x}_2, \tilde{x}_4, \tilde{x}_5)$ are now decoupled from those of altitude $(\tilde{x}_3, \tilde{x}_6)$. Indeed, $\tilde{x}_3$ and $\tilde{x}_6$ have simple linear dynamics that can be controlled with any standard linear control techniques. The variables $\tilde{x}_1, \tilde{x}_2, \tilde{x}_3$, and $\tilde{x}_4$, instead, have nonlinear dynamics described by a time-varying system that depends on the yaw angle $\psi$. A straightforward and indeed physically meaningful way of solving this nonlinear control problem is through this choice of the following control inputs:

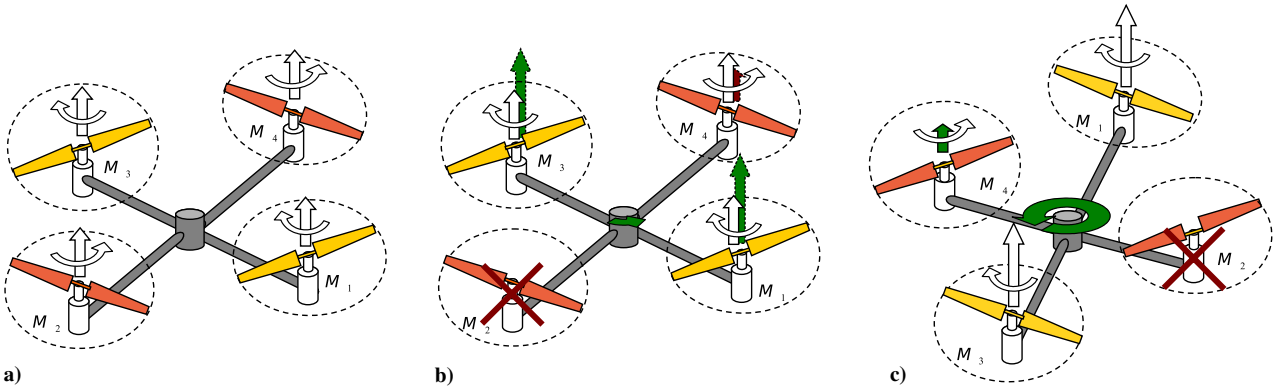


**Fig. 5 Quadrotor vehicle experiencing a fault on motor 2.**

**Table 1 Quadrotor and controller parameters**

| | Value | Unit | Description |
|---|---|---|---|
| $m$ | 0.5 | kg | Quadrotor mass |
| $g$ | 9.81 | m/s$^2$ | Gravity acceleration |
| $I_{xx}$ | $5.9 \times 10^{-3}$ | kg · m$^2$ | Inertia coefficient along $x_B$ axis |
| $I_{yy}$ | $5.9 \times 10^{-3}$ | kg · m$^2$ | Inertia coefficient along $y_B$ axis |
| $I_{zz}$ | $1.16 \times 10^{-3}$ | kg · m$^2$ | Inertia coefficient along $z_B$ axis |
| $l$ | 0.255 | m | Distance between rotor and c.g. |
| $d$ | $2.4 \times 10^{-3}$ | kg · m$^2$ | Ratio between blade drag and thrust coefficients |

**Table 2 Initial conditions for the inner control loop simulation**

| | Value | Unit | Description |
|---|---|---|---|
| $x_1$ | $-\pi/4$ | rad | $\phi$ |
| $x_2$ | $\pi/4$ | rad | $\theta$ |
| $x_3$ | $\pi/4$ | rad | $\psi$ |
| $x_4$ | $-0.5$ | rad/s | $p$ |
| $x_5$ | 0.5 | rad/s | $q$ |
| $x_6$ | 2.7 | rad/s | $r$ |

$$\begin{bmatrix} \tilde{u}_1 \\ \tilde{u}_2 \end{bmatrix} = \begin{bmatrix} S_\psi & C_\psi \\ -C_\psi & S_\psi \end{bmatrix}^T \begin{bmatrix} \tilde{\tilde{u}}_1 \\ \tilde{\tilde{u}}_2 \end{bmatrix} \tag{31}$$

because this control input (31) reduces Eqs. (30d) and (30e) to

$$\dot{\tilde{x}}_4 = \tilde{\tilde{u}}_1 - \frac{k_t}{m}\tilde{x}_4 \tag{32a}$$

$$\dot{\tilde{x}}_5 = \tilde{\tilde{u}}_2 - \frac{k_t}{m}\tilde{x}_5 \tag{32b}$$

where $\tilde{\tilde{u}}_1$ and $\tilde{\tilde{u}}_2$ represent the control inputs for the linear system (32a) and (32b) with Eqs. (30a) and (30b). These resulting linear dynamics can then again be controlled using any simple standard linear control technique. Once $\tilde{u}_1$, $\tilde{u}_2$, and $\tilde{u}_3$ are calculated, it is possible to compute the desired values of $x_{1,d}$, $x_{2,d}$, and $x_{6,d}$ from Eq. (29b) to use as set points for the inner control loop. Note that $x_{6,d}$ is close to $mgd/k_r$ (and hence $\tilde{u}_3$ is close to $g$), whereas $x_{1,d}$ and $x_{2,d}$ are small angles.

The outer controller generates time-varying outputs, which are references to the inner control loop, because these reference signals depend on a rotation matrix of the vehicle yaw angle. Because the quadrotor, due to rotor failure, is spinning around its yaw axis, it is necessary to periodically cycle the inner control loop set points generated by the outer control loop to achieve the desired translation movements in the Earth-fixed reference frame, with a frequency and phase that must be synchronized with the heading of the spinning vehicle. All of this is achieved through the rotation matrix in Eq. (31), which depends on the yaw angle $\psi$ and the mapping of the linear control inputs $\tilde{\tilde{u}}_1$ and $\tilde{\tilde{u}}_2$ via this rotation matrix to the periodic cyclic time-varying control inputs $\tilde{u}_1$ and $\tilde{u}_2$. Using the outer controller together with the inner controller, it is then possible to decide the Earth frame position where the quadcopter can translate to and perhaps land (if desired).

### 3. *Physical Considerations*

The proposed control law exploits the conservation of the angular momentum around the vertical axis of the quadrotor. When one of the rotors fails, (e.g., rotor 2 in Fig. 5b), the speed of the rotor laying on the opposite end of the faulty rotor is modulated until the value of the angle of inclination of the vehicle from the horizontal plane converges to zero. When this is achieved (Fig. 5c), the healthy rotor of

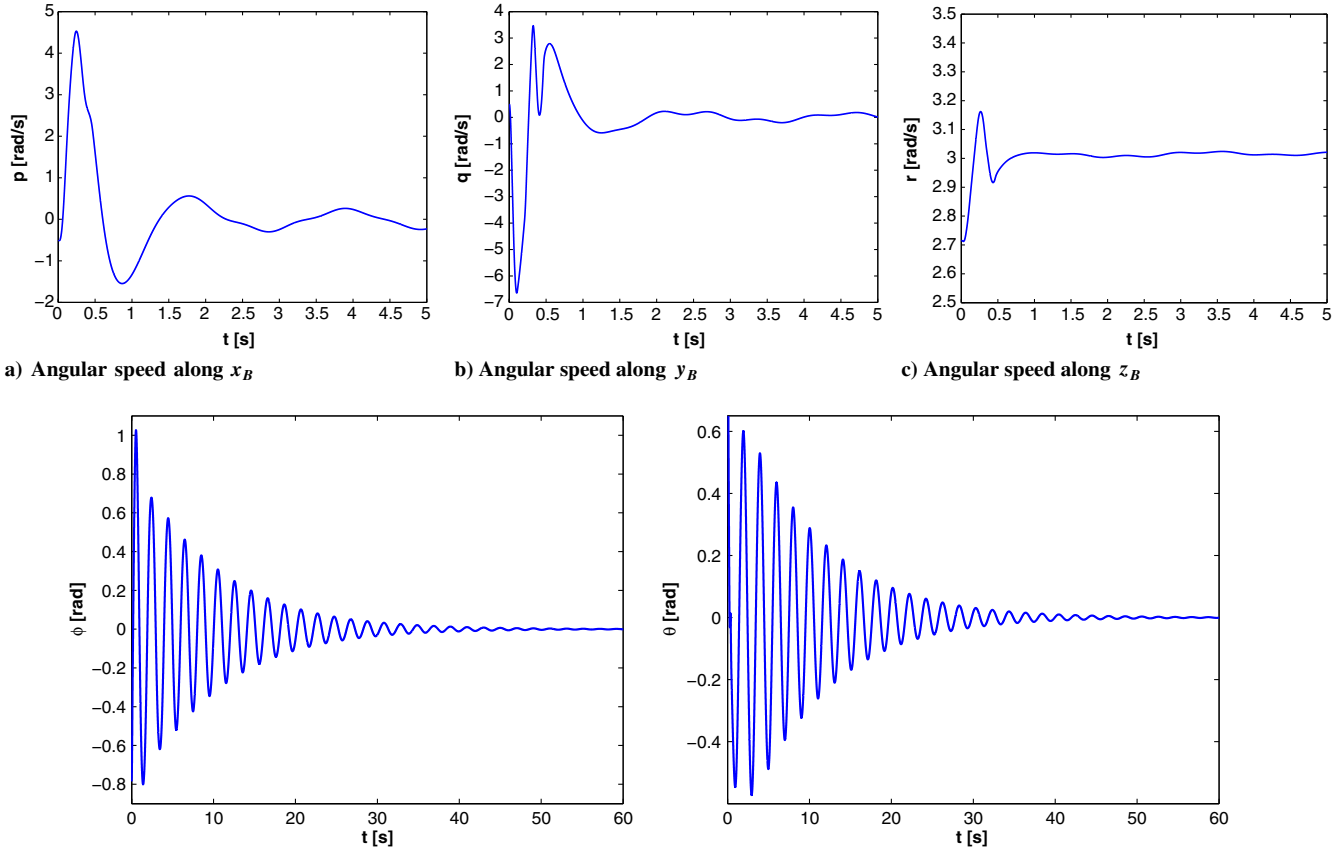


a) Angular speed along $x_B$ b) Angular speed along $y_B$ c) Angular speed along $z_B$

d) Roll angle $\phi$ e) Pitch angle $\theta$

**Fig. 6 Angular dynamics of the closed-loop system (inner control loop with saturation and rate limiting).**

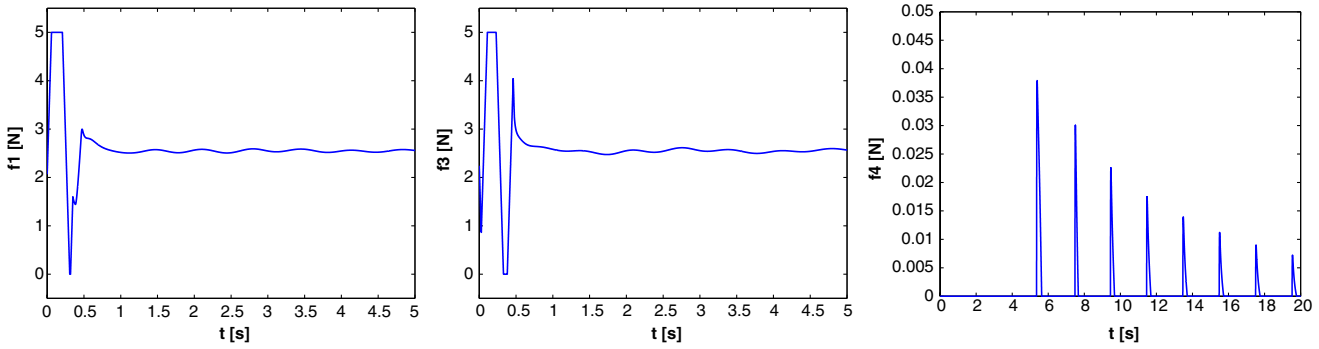


a) Rotor force $f_1$ b) Rotor force $f_3$ c) Rotor force $f_4$

**Fig. 7 Rotor forces required by the inner control loop to stabilize the quadrotor.**



the faulty couple supplies an almost zero thrust, and the lift thrust necessary to cancel out the gravity force must be supplied by the healthy couple of rotors. In this configuration, the quadrotor is parallel to the ground, spinning around the vertical axis with a steady-state rotational velocity depending on the rotational drag. Varying simultaneously the rotational velocity of the two rotors of the healthy couple, it is also possible to set a desired altitude for the vehicle. Once the vehicle is spinning around its vertical axis, it is possible to supply a proper cyclic periodic control input to the healthy couple of rotors to make the quadrotor reach any desired position in 3-D space. The control law needs only to modify the desired direction of the total lift thrust, because the motion in 3-D space depends on that direction. Because the vehicle rotates around its yaw axis, to keep the total lift thrust at a desired direction, it is necessary to vary each motor thrust with a synchronized frequency and phase proportional to the vehicle yaw angular velocity at which the vehicle is rotating.

When both the inner and outer control loops are running, the quadrotor can remain parallel to the ground spinning on its vertical axis, using only the two motors mounted opposite each other on opposite arms, and move to a desired position in 3-D space, applying a pseudoperiodic lift thrust to each functional rotor, with the same frequency and phase as the rotational velocity.

When the quadrotor touches the ground, the angular velocity $r$ must be limited to avoid possible damages to the vehicle. It may be sensible to equip the undercarriage of the quadrotor with unactuated free rotative wheels.

## IV. Simulation Results

The developed control strategy is capable of stabilizing the quadrotor roll and pitch angles and to perform 3-D position control. As previously anticipated in Sec. II.B, the higher fidelity verification model used in the simulator includes blade gyroscopic effect, actuators saturation, and rate limiting. Blade gyroscopic effect can be seen as a model uncertainty (i.e., an effect that has not been taken into account for synthesizing the control law, but which is present in the real system). Saturations and rate limiters, instead, can be seen as actuator uncertainties. This section shows the behavior of the system controlled by the inner control loop first and by both the control loops afterward, when both model and actuator uncertainties are taken into account. The simulation system consists of three modules:

1) The nonlinear system module includes all the differential equations described in Sec. II (rigid body dynamics, drag, and blade gyroscopic effect).

2) The nonlinear controller module includes the equations described in Sec. III.

3) A constraint module that contains actuators saturation and rate limiting.

In the present section, the results of two different simulations are reported. Both simulations have been performed with the controllers activated at $t = 0$ and using the parameters reported in Table 1.

### A. Inner Control Loop Simulation

In the first simulation scenario, only the inner control loop is activated, and it must stabilize the roll and pitch angles (i.e., $x_{1,d} \to 0$, $x_{2,d} \to 0$) while regulating the angular speed $r$ at a desired value (chosen to be the steady-state value at which the quadrotor retains an arbitrary constant altitude, i.e., $x_{6,d} \to mgd/k_r$). The simulation has been run for 60 s, saturation and rate-limiting constraints have been included in the simulation scenario ($f_{\max} = 5$ N, $f_{\min} = 0$ N, $\Delta f = 50$ N/s), and the initial conditions are reported in Table 2.

The angular speeds around $x_B$, $y_B$, and $z_B$ axes, together with the values of roll and pitch angles, are reported in Fig. 6. The rotor forces requested by the inner control law exceed the admissible upper (5 N) and lower (0 N) saturation levels and hence saturate at 5 and 0 N, respectively, as shown in Fig. 7; nevertheless, the states reach their desired values at steady state.

### B. Outer Control Loop

In the second simulation scenario, both the inner and outer control loops are activated. The controller must fly the quadrotor vehicle from its initial position to $x = 0$ and $y = 0$ of the Earth frame, staying in hover flight above $x = 0$, $y = 0$ at $z = 1$ m (i.e., $x_{7,d} = x_d \to 0$, $x_{8,d} = y_d \to 0$, and $x_{9,d} = z_d \to 1$). This represents a possible real scenario, where the quadrotor experiences a problem to a rotor, switches that rotor off and moves back to its recovery base, which is here assumed to be at the origin.

The simulation has been run for 60 s, saturation and rate-limiting constraints have been included in the simulation scenario ($f_{\max} = 5$ N, $f_{\min} = 0$ N, $\Delta f = 50$ N/s) and the initial conditions are reported in Table 3.

The quadrotor position in 3-D space is reported in Fig. 8. The rotor forces requested by the control law exceed again the admissible upper (5 N) and lower (0 N) saturation levels and hence are saturated at these upper and lower limits, as shown in Fig. 9; nevertheless, the states reach their desired values at steady state. As already described in

**Table 3 Initial conditions for the outer control loop simulation**

| | Value | Unit | Description |
|---|---|---|---|
| $x_1$ | 0.075 | rad | $\phi$ |
| $x_2$ | 0.025 | rad | $\theta$ |
| $x_3$ | 0.1 | rad | $\psi$ |
| $x_4$ | 0.03 | rad/s | $p$ |
| $x_5$ | 0.02 | rad/s | $q$ |
| $x_6$ | 2.7 | rad/s | $r$ |
| $x_7$ | 5 | m | $x$ |
| $x_8$ | 5 | m | $y$ |
| $x_9$ | 5 | m | $z$ |
| $x_{10}$ | 0 | m/s | $\dot{x}$ |
| $x_{11}$ | 0 | m/s | $\dot{y}$ |
| $x_{12}$ | 0 | m/s | $\dot{z}$ |

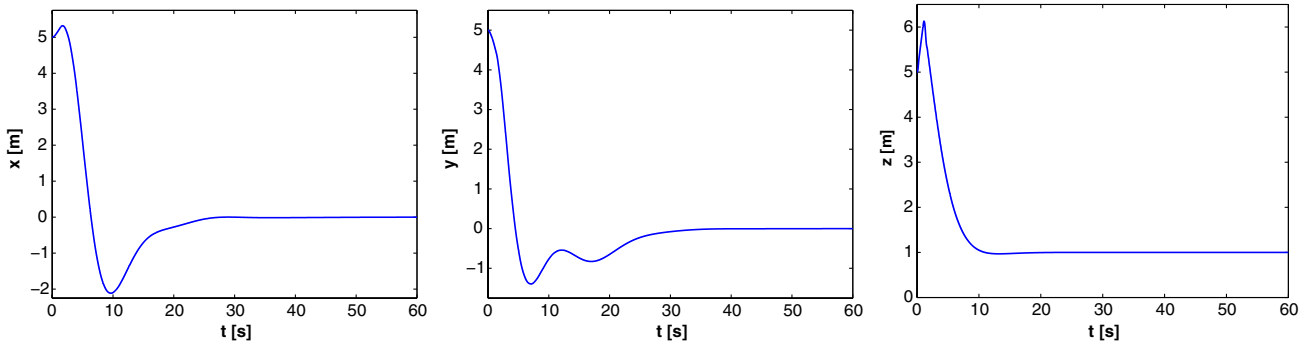


a) Longitudinal displacement $x$ b) Lateral displacement $y$ c) Vertical displacement $z$

**Fig. 8 Position in 3-D space (inner and outer control loops with saturation and rate limiting).**

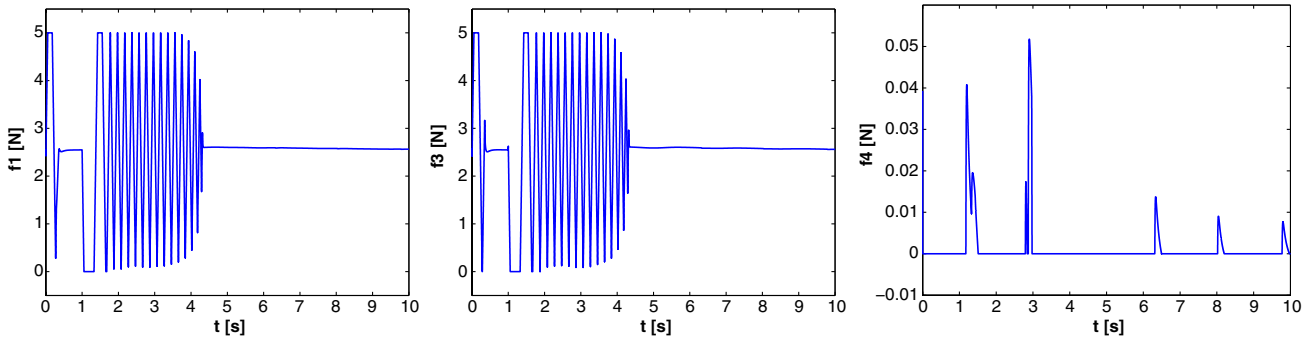


a) Rotor force $f_1$ b) Rotor force $f_3$ c) Rotor force $f_4$

**Fig. 9 Rotor forces required by the double-loop architecture to perform trajectory following.**

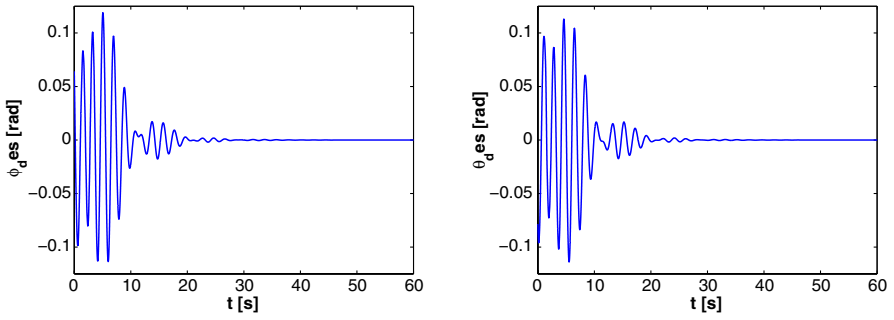


a) Desired value of roll generated by the outer controller $x_{1,d}$ b) Desired value of pitch generated by the outer controller $x_{2,d}$

**Fig. 10 Desired values of roll and pitch generated by the outer control.**

Sec. III.C.2, the roll and pitch reference generated by the outer controller is cyclic, and this is illustrated in Fig. 10.

## V. Conclusions

The present paper deals with the problem of controlling a quadrotor aerial vehicle when one of the actuators/rotors is no longer capable of supplying thrust (e.g., propeller loss, electrical or mechanical actuator failure). The problem is solved using a double control loop architecture in which model-based techniques are adopted in both control loops.

The developed control laws exploit the conservation of angular momentum around the vertical axis of the quadrotor. The only loss in control is the yaw angle, because the vehicle is made to enter a yaw constant angular velocity spin by the designed control law. This aspect is not problematic for vehicle safety, though it does limit the ability for the vehicle to point any visual sensor in a desired direction. However, this is a minor loss because it is already a significant achievement to keep the vehicle flying in the air with only three functional rotors.

Once the vehicle has entered a constant yaw angular velocity spin, it is possible to provide a cyclic reference in desired roll and pitch angles to make it translate to a desired position to 3-D space. The period of each cyclic reference depends on the steady-state value of the yaw angular speed, which is related to the vehicle mass, drag, blade drag, and thrust coefficients.

For this architecture to be applied on a real vehicle, however, the following points should be considered.

The motors should be capable of providing the maximum thrust required by the control law and this has to be compatible with the size and energy requirements of the vehicle. The minimum theoretical maximal thrust that must be provided by each motor is equal to $1/2$ mg because, at steady state, only two rotors are working to compensate for the gravitational force. Simulation results showed that, if the user wishes to have a fast transient, it is necessary to have generous actuator saturation levels, with a good rule-of-thumb represented by a saturation level equal to the quadrotor weight.

Maximum thrust is not the only property that should be taken into account when choosing the motors. Motors should also be chosen to

provide the maximum angular acceleration (thrust rate), and this should be compatible with the size and energy requirements of the vehicle. Vehicle stabilization requires the rotor that is opposed to the failed actuator to provide a pulse-like thrust. It is thus important that the thrust reference generated by the control law can be followed quickly by the motor. Simulation results showed that, to retain stability and have a quick transient response, a good rule-of-thumb choice is represented by a rate limiter, which allows the saturation level to be reached in tenths of seconds.

Finally, the control hardware should be chosen to have enough computational power to run the proposed control algorithms. The computational requirements of the proposed solution are actually being investigated through hardware-in-the-loop simulations by the authors. This should not be a big limitation because modern embedded electronic microcontrollers can perform fast floating point arithmetic.

Notwithstanding the fact that the proposed approach has been tested in simulation only and the FDI problem has not been directly addressed, the authors believe that the proposed control scheme presented in this paper lays down the important conceptual foundations for subsequent robust fault tolerant control designs in the presence of actuator failure, and shows, for the very first time, that a quadrotor can maintain stable controlled flight with only three functional rotors. This work shows that, by spinning the vehicle in the yaw direction and maintaining roll and pitch torque control, actuators can be cycled to obtain full translational control.

## Appendix: The Robust Feedback Linearizing Control Law

The robust feedback linearizing control law (20) for system (23) is given by

$$\begin{aligned}\hat{\boldsymbol{u}}(\hat{\boldsymbol{x}}, \boldsymbol{v}) &= \boldsymbol{\alpha}(\hat{\boldsymbol{x}}) + \boldsymbol{\beta}(\hat{\boldsymbol{x}})v \\ &= [\,\alpha_1(\hat{\boldsymbol{x}}) \quad \alpha_2(\hat{\boldsymbol{x}}) \quad \alpha_3(\hat{\boldsymbol{x}})\,]^T + \boldsymbol{\beta}(\hat{\boldsymbol{x}})[\,v_1 \quad v_2 \quad v_3\,]^T\end{aligned}$$

where

$$\begin{aligned}
\alpha_1(\boldsymbol{x}) &= -2lI_{zz}k_r^2\Bigg(I_{xx}\Bigg(-\frac{1}{4}C_{\hat{x}_2}^{-2}I_{zz}(2d^2g^2m^2(S_{2\hat{x}_1}+\hat{x}_1+C_{2\hat{x}_2}(-4S_{\hat{x}_1}+\hat{x}_1)-S_{2\hat{x}_2}\hat{x}_2T_{\hat{x}_1})+\\
&\quad 2dgmk_r(-3\hat{x}_4-4C_{2\hat{x}_2}S_{\hat{x}_1}\hat{x}_5+C_{\hat{x}_1}^{-1}(2\hat{x}_4-C_{3\hat{x}_1}\hat{x}_4+2C_{2\hat{x}_1}C_{2\hat{x}_2}\hat{x}_4+S_{3\hat{x}_1}\hat{x}_5)+\\
&\quad +(2S_{2\hat{x}_2}\hat{x}_3+\hat{x}_5)T_{\hat{x}_1})++k_r^2(-6\hat{x}_4\hat{x}_5-C_{\hat{x}_1}^{-1}(2S_{2\hat{x}_2}\hat{x}_3\hat{x}_4+2C_{3\hat{x}_1}\hat{x}_4\hat{x}_5+S_{3\hat{x}_1}(\hat{x}_4-\hat{x}_5)(\hat{x}_4+\hat{x}_5))+\\
&\quad +(\hat{x}_5^2-3\hat{x}_4^2+2C_{2\hat{x}_2}\hat{x}_4^2)\cdot T_{\hat{x}_1}))-C_{\hat{x}_1}^{-1}k_r^3\hat{x}_5T_{\hat{x}_2})+I_{zz}(k_r^2(C_{\hat{x}_1}^{-1}k_r\hat{x}_5T_{\hat{x}_2}-dgm(\hat{x}_2+\\
&\quad +C_{\hat{x}_1}^{-1}(-1+S_{\hat{x}_1}\hat{x}_1)T_{\hat{x}_2}))++I_{zz}(-k_r^2\hat{x}_4\hat{x}_5+dgmk_r(-\hat{x}_4+C_{\hat{x}_1}\hat{x}_4-S_{\hat{x}_1}\hat{x}_5+\hat{x}_3T_{\hat{x}_1}T_{\hat{x}_2}+\\
&\quad +S_{\hat{x}_1}(\hat{x}_5+\hat{x}_4T_{\hat{x}_1})T_{\hat{x}_2}^2)+d^2g^2m^2\cdot(\hat{x}_1-\hat{x}_2T_{\hat{x}_1}T_{\hat{x}_2}+S_{\hat{x}_1}(-1+T_{\hat{x}_2}^2)))\Bigg)\Bigg),\\
\alpha_2(\boldsymbol{x}) &= I_{zz}k_r^2(I_{xx}(-k_r^3\hat{x}_5T_{\hat{x}_1}+I_{zz}(d^2g^2m^2(C_{\hat{x}_1}^{-1}\hat{x}_2+(-2+C_{\hat{x}_1})T_{\hat{x}_2})+k_r^2(\hat{x}_3(2\hat{x}_5+\hat{x}_4T_{\hat{x}_1})+\\
&\quad +C_{\hat{x}_1}^{-1}(S_{\hat{x}_1}\hat{x}_4+C_{\hat{x}_1}\hat{x}_5)^2T_{\hat{x}_2})+2dgmk_r(\hat{x}_3-C_{\hat{x}_1}^{-1}\hat{x}_3+(S_{\hat{x}_1}\hat{x}_4-\hat{x}_5+C_{\hat{x}_1}\hat{x}_5-\hat{x}_4T_{\hat{x}_1})T_{\hat{x}_2})))+\\
&\quad +I_{zz}(C_{\hat{x}_1}^{-1}k_r^2(dgm(S_{\hat{x}_1}-\hat{x}_1)+S_{\hat{x}_1}k_r\hat{x}_5)+I_{zz}(-k_r^2\hat{x}_3\hat{x}_5+d^2g^2m^2(-C_{\hat{x}_1}^{-1}\hat{x}_2+T_{\hat{x}_2})+\\
&\quad +dgmk_r((-1+C_{\hat{x}_1}^{-1})\hat{x}_3+(\hat{x}_5+\hat{x}_4T_{\hat{x}_1})T_{\hat{x}_2})))),\\
\alpha_3(x) &= 0,\\
\boldsymbol{\beta}(\boldsymbol{x}) &= \begin{pmatrix} 1 & -\frac{2T_{\hat{x}_1}T_{\hat{x}_2}}{l} & -\frac{2C_{\hat{x}_1}^{-1}I_{xx}T_{\hat{x}_2}}{lI_{zz}} \\ 0 & SC_{\hat{x}_1} & \frac{I_{xx}T_{\hat{x}_1}}{I_{zz}} \\ 0 & 0 & 1 \end{pmatrix}
\end{aligned}$$

## References


[1] Hoffmann, G., Huang, H., Waslander, S., and Tomlin, C., "Quadrotor Helicopter Flight Dynamics and Control: Theory and Experiment," *Proceedings of the AIAA Guidance, Navigation, and Control Conference*, Vol. 4, Hilton Head, SC, Aug. 2007, pp. 44–48.

[2] Prior, S., Shen, S., Karamanoglu, M., Odedra, S., Erbil, M., Barlow, C., and Lewis, D., "Future of Battlefield Micro Air Vehicle Systems," *Proceedings of the International Conference on Manufacturing and Engineering Systems*, National Formosa University, Huwei, Taiwan,, Dec. 2009, pp. 374–379.

[3] Das, A., Subbarao, K., and Lewis, F., "Dynamic Inversion with Zero-Dynamics Stabilisation for Quadrotor Control," *IET Control Theory Applications*, Vol. 3, No. 3, March 2009, pp. 303–314. doi: 10.1049/iet-cta:20080002

[4] Voos, H., "Nonlinear Control of a Quadrotor Micro-UAV Using Feedback-Linearization," *Proceedings of the IEEE International Conference on Mechatronics (ICM)*, IEEE, Piscataway, NJ, April 2009, pp. 1–6.

[5] Pettazzi, L., Lanzon, A., Theil, S., and Ercoli Finzi, A., "Design of Robust Drag-Free Controllers with Given Structure," *Journal of Guidance, Control, and Dynamics*, Vol. 32, No. 5, 2009, pp. 1609–1621. doi: 10.2514/1.40279

[6] Crowther, B., Lanzon, A., Maya-Gonzalez, M., and Langkamp, D., "Kinematic Analysis and Control Design for a Nonplanar Multirotor Vehicle," *Journal of Guidance, Control, and Dynamics*, Vol. 34, No. 4, 2011, pp. 1157–1171. doi: 10.2514/1.51186

[7] Hess, R., and Bakhtiari-Nejad, M., "Sliding-Mode Control of a Nonlinear Model of an Unmanned Aerial Vehicle," *Journal of Guidance, Control, and Dynamics*, Vol. 31, No. 4, 2008, pp. 1163–1166. doi: 10.2514/1.32558

[8] Castillo, P., Lozano, R., and Dzul, A., "Modelling and Control of Mini-Flying Machines," 1st ed., Springer–Verlag, New York, 2005, pp. 39–59.

[9] Kendoul, F., Lara, D., Fantoni-Coichot, I., and Lozano, R., "Real-Time Nonlinear Embedded Control for an Autonomous Quadrotor Helicopter," *Journal of Guidance, Control, and Dynamics*, Vol. 30, No. 4, 2007, pp. 1049–1061. doi: 10.2514/1.27882

[10] Lee, D., Kim, H., and Sastry, S., "Feedback Linearization vs. Adaptive Sliding Mode Control for a Quadrotor Helicopter," *International Journal of Control, Automation and Systems*, Vol. 7, No. 3, June 2009, pp. 419–428. doi: 10.1007/s12555-009-0311-8

[11] Bouabdallah, S., and Siegwart, R., "Full Control of a Quadrotor," *Proceedings of IEEE/RSJ International Conference on Intelligent*

*Robots and Systems (IROS)*, IEEE, Piscataway, NJ, Oct.–Nov. 2007, pp. 153–158.

[12] Raffo, G., Ortega, M., and Rubio, F., "Integral Predictive/Nonlinear $H_\infty$ Control Structure for a Quadrotor Helicopter," *Automatica*, Vol. 46, No. 1, 2010, pp. 29–39. doi: 10.1016/j.automatica.2009.10.018

[13] Slegers, N., Kyle, J., and Costello, M., "Nonlinear Model Predictive Control Technique for Unmanned Air Vehicles," *Journal of Guidance, Control, and Dynamics*, Vol. 29, No. 5, 2006, pp. 1179–1188. doi: 10.2514/1.21531

[14] Zhou, Q.-L., Zhang, Y., Rabbath, C., and Theilliol, D., "Design of Feedback Linearization Control and Reconfigurable Control Allocation with Application to a Quadrotor UAV," *Proceedings of the Conference on Control and Fault-Tolerant Systems (SysTol)*, IEEE, Nice, Oct. 2010, pp. 371–376.

[15] Sharifi, F., Mirzaei, M., Gordon, B., and Zhang, Y., "Fault Tolerant Control of a Quadrotor UAV Using Sliding Mode Control," *Proceeding of the Conference on Control and Fault-Tolerant Systems (SysTol)*, IEEE, Nice, Oct. 2010, pp. 239–244.

[16] Izadi, H., Zhang, Y., and Gordon, B., "Fault Tolerant Model Predictive Control of Quad-Rotor Helicopters with Actuator Fault Estimation," *Proceedings of the 18th IFAC World Congress*, Vol. 18, No. 1, Aug.–Sept. 2011, pp. 6343–6348.

[17] Franco, A., Bourles, H., De Pieri, E., and Guillard, H., "Robust Nonlinear Control Associating Robust Feedback Linearization and $H_\infty$ Control," *IEEE Transactions on Automatic Control*, Vol. 51, No. 7, 2006, pp. 1200–1207. doi: 10.1109/TAC.2006.878782

[18] Mokhtari, A., Benallegue, A., and Daachi, B., "Robust Feedback Linearization and $H_\infty$ Controller for a Quadrotor Unmanned Aerial Vehicle," *Proceedings of the IEEE/RSJ International Conference on Intelligent Robots and Systems (IROS)*, IEEE, Aug. 2005, pp. 1198–1203.

[19] Kendoul, F., Lara, D., Fantoni, I., and Lozano, R., "Nonlinear Control for Systems with Bounded Inputs: Real-Time Embedded Control Applied to UAVS," *Proceedings of the IEEE Conference on Decision and Control (CDC)*, IEEE, Piscataway, NJ, Dec. 2006, pp. 5888–5893.

[20] Raffo, G. V., Ortega, M. G., and Rubio, F. R., "Backstepping/Nonlinear $H_\infty$ Control for Path Tracking of a Quadrotor Unmanned Aerial Vehicle," *American Control Conference (ACC)*, IEEE, Seattle, WA , June 2008, pp. 3356–3361.

[21] Madani, T., and Benallegue, A., "Control of a Quadrotor Mini-Helicopter via Full State Backstepping Technique," *Proceedings of the IEEE Conference on Decision and Control*, IEEE, Piscataway, NJ, Dec. 2006, pp. 1515–1520.

[22] Bouabdallah, S., Murrieri, P., and Siegwart, R., "Design and Control of an Indoor Micro Quadrotor," *Proceedings of IEEE International Conference on Robotics and Automation (ICRA)*, Vol. 5, IEEE, Piscataway, NJ, April–May 2004, pp. 4393–4398.

[23] Pounds, P., Mahony, R., and Corke, P., "Modelling and Control of a Large Quadrotor Robot," *Control Engineering Practice*, Vol. 18, No. 7, 2010, pp. 691–699. doi: 10.1016/j.conengprac.2010.02.008

[24] Fossen, T., *Marine Control Systems: Guidance, Navigation and Control of Ships, Rigs and Underwater Vehicles*, 1st ed., Marine Cybernetics, Trondheim, Norway, 2002, pp. 17–63.

[25] Freddi, A., Lanzon, A., and Longhi, S., "Feedback Linearization Approach to Fault Tolerance in Unmanned Quadrotor Vehicles," *Proceedings of the 18th IFAC World Congress*, Vol. 8, No. 1, Aug.–Sept. 2011, pp. 5413–5418.

[26] Bouadi, H., Bouchoucha, M., and Tadjine, M., "Modelling and Stabilizing Control Laws Design Based on Sliding Mode for an UAV Type-Quadrotor," *Engineering Letters*, Vol. 15, No. 2, 2007, pp. 342–347.

[27] Tayebi, A., and McGilvray, S., "Attitude Stabilization of a VTOL Quadrotor Aircraft," *IEEE Transactions on Control Systems Technology*, Vol. 14, No. 3, 2006, pp. 562–571. doi: 10.1109/TCST.2006.872519

[28] Ding, S., *Model-Based Fault Diagnosis Techniques: Design Schemes, Algorithms, and Tools*, Springer–Verlag, New York, 2008, pp. 71–114.

[29] Ranjbaran, M., and Khorasani, K., "Fault Recovery of an Under-Actuated Quadrotor Aerial Vehicle," *49th IEEE Conference on Decision and Control (CDC)*, IEEE, Piscataway, NJ, Dec. 2010, pp. 4385–4392.

[30] Freddi, A., Longhi, S., and Monteriu, A., "Actuator Fault Detection System for a Mini-Quadrotor," *Proceedings of the 2010 IEEE International Symposium on Industrial Electronics (ISIE)*, IEEE, Piscataway, NJ, July 2010, pp. 2055–2060.

[31] Isidori, A., "Nonlinear Control Systems," Vol. 1, Springer–Verlag, 1995, pp. 219–241.

[32] Guillard, H., and Bourles, H., "Robust Feedback Linearization," *Proceedings of the 14th International Symposium Mathematical Theory of Networks and Systems (MTNS)*, June 2000, pp. 1–6.

[33] Lanzon, A., "Weight Optimisation in $H_\infty$ Loop-Shaping," *Automatica*, Vol. 41, No. 7, 2005, pp. 1201–1208. doi: 10.1016/j.automatica.2005.01.010